Environmental Science & Technology

pubs.acs.org/est

Article

Stability of Monoterpene-Derived α-Hydroxyalkyl-Hydroperoxides in Aqueous Organic Media: Relevance to the Fate of Hydroperoxides in Aerosol Particle Phases

Junting Qiu, Zhancong Liang, Kenichi Tonokura, Agustín J. Colussi,* and Shinichi Enami*

Cite This: *Environ. Sci. Technol.* 2020, 54, 3890−3899

Read Online

ACCESS | Metrics & More | Article Recommendations | Supporting Information

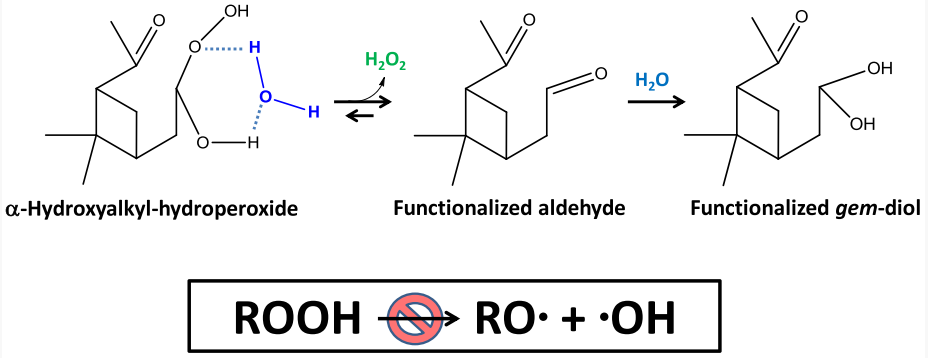

ABSTRACT: The α-hydroxyalkyl-hydroperoxides [R−(H)C(−OH)(−OOH), α-HH] produced in the ozonolysis of unsaturated organic compounds may contribute to secondary organic aerosol (SOA) aging. α-HHs' inherent instability, however, hampers their detection and a positive assessment of their actual role. Here we report, for the first time, the rates and products of the decomposition of the α-HHs generated in the ozonolysis of atmospherically important monoterpenes α-pinene (α-P), *d*-limonene (*d*-L), γ-terpinene (γ-Tn), and α-terpineol (α-Tp) in water/acetonitrile (W/AN) mixtures. We detect α-HHs and multifunctional decomposition products as chloride adducts by online electrospray ionization mass spectrometry. Experiments involving D_2O and $H_2{}^{18}O$, instead of $H_2{}^{16}O$, and an OH-radical scavenger show that α-HHs decompose into *gem*-diols + H_2O_2 rather than free radicals. α-HHs decay mono- or biexponentially depending on molecular structure and solvent composition. e-Fold times, $\tau_{1/e}$, in water-rich solvent mixtures range from $\tau_{1/e}$ = 15−45 min for monoterpene-derived α-HHs to $\tau_{1/e} > 10^3$ min for the α-Tp-derived α-HH. All $\tau_{1/e}$'s dramatically increase in <20% (v/v) water. Decay rates of the α-Tp-derived α-HH in pure water increase at lower pH (2.3 ≤ pH ≤ 3.3). The hydroperoxides detected in day-old SOA samples may reflect their increased stability in water-poor media and/or the slow decomposition of α-HHs from functionalized terpenes.

INTRODUCTION

The detection of extremely low-volatility organic compounds (ELVOCs)[1−3] has gone a long way to explaining how biogenic volatile organic compounds (VOCs) contribute to the formation of secondary organic aerosol (SOA).[4,5] ELVOCs are mostly produced during the ozonolysis of monoterpenes ($C_{10}H_{16}$), particularly those containing endocyclic double bonds such as α-pinene (see Scheme 1),[2,6] and condense as nanoparticles. High-resolution chemical ionization mass spectrometry reveals that α-pinene ELVOCs consist of highly oxidized monomeric $C_{x=8-10}H_{y=12-16}O_{z=6-12}$ and dimeric $C_{x=17-20}H_{y=26-32}O_{z=8-18}$ species.[1,3] The mechanism of ELVOCs formation involves Criegee intermediates (CIs) that isomerize, fragment, or undergo reactions with hydroxylic species such acids, alcohols, and water.[7−10] The fragmentation of CIs produces alkylperoxyl (R′OO·) radicals that undergo fast intramolecular H-transfers into hydroperoxides and

Scheme 1. Chemical Structures of the Monoterpenes Used in the Present Study

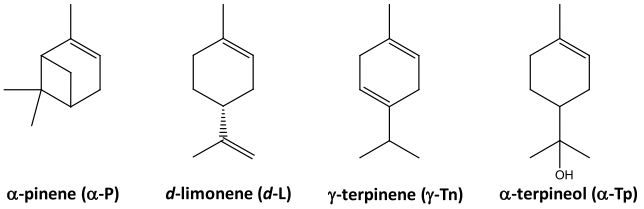

Received: December 9, 2019
Revised: February 28, 2020
Accepted: March 4, 2020
Published: March 4, 2020

https://dx.doi.org/10.1021/acs.est.9b07497
Environ. Sci. Technol. 2020, 54, 3890−3899

second-generation R″OO· radicals.[11,12] The latter propagate an autoxidation mechanism that produces ELVOCs possessing multiple hydroperoxide functionalities and elevated O/C ratios.[13−15] CIs also react with water yielding α-hydroxyalkyl-hydroperoxides (R−(H)C(−OOH)(−OH), α-HHs).[7,14]

Hydroperoxides as a class are thermally unstable[16−18] and decompose into RO· and HO· radicals via O−O homolysis.[19,20] On this basis, it was hypothesized that they could trigger SOA aging via free radical reactions under atmospheric conditions. Previous kinetic studies, however, show that alkyl hydroperoxides in dilute solutions decompose at high temperatures, having $\tau_{1/2}$ = 10 h half-lives above 130 °C.[18] The unidentified (hydro)peroxide functionalities contained in the highly oxygenated molecules (HOMs) produced in the ozonolysis of α-pinene (quantified by iodometry),[21] however, decompose (into unidentified products) in tens of minutes at ambient temperature.[22]

Clearly, a better understanding of the factors that control the stabilities of hydroperoxides and the identity of their decomposition products in condensed phases will help assess their actual role in SOA chemistry and, as potential sources of reactive oxygen species (ROS), the toxicity of ambient particulate matter.[23] Here, we investigate the products and decomposition rates of four atmospherically relevant monoterpene-derived α-HHs in aqueous organic solutions at ambient temperature for the first time. Since α-HHs are the least stable hydroperoxides,[18] their lifetimes should provide a lower bound to the lifetimes of hydroperoxides, and insights into structural and matrix effects on α-HHs' persistence.

Recently, we found that the α-HHs generated from the ozonolysis of the sesquiterpene β-caryophyllene in water/acetonitrile (W/AN) mixtures containing NaCl (an inert cosolute that does not react with O_3 during our experiments) could be detected as chloride adducts by electrospray ionization mass spectrometry (ESI-MS).[24,25] The same study showed that α-HHs decay in a couple of hours in ≥20% (v/v) water mixtures but persist longer than a day in <10 vol % water.[25] The goal of the present study is to investigate the effects of chemical structure and other functional groups on the stability of α-HHs. This information may help evaluate the fate of atmospherically relevant α-HHs in general. Here we report the rates of decomposition of α-HHs produced in the ozonolysis of α-pinene (α-P), *d*-limonene (*d*-L), γ-terpinene (γ-Tn), and α-terpineol (α-Tp) (Scheme 1) in W/AN mixtures of variable compositions. Our study focuses on α-P as the most abundant biogenic monoterpene, whose global annual emissions (66.1 Tg) vastly exceed those of related β-pinene (18.9 Tg) and limonene (11.4 Tg).[26] We take advantage of the high solubility of α-Tp in pure water to investigate the effects of pH on α-HH decay rates. The main findings are that in aqueous organic media monoterpene α-HHs decompose into hydrogen peroxide plus aldehydes rather than free radicals in tens of minutes, with e-fold decay times, $\tau_{1/e}$, that depend sensitively on water content and the presence of substituents. The fact that $\tau_{1/e}$'s depend nonlinearly on water content for all tested terpenes strongly suggests that similar behaviors should be expected for the α-HHs produced in aqueous media in the atmosphere. We found that the decomposition of the α-Tp-derived α-HH in water is accelerated at lower pH in the range of acidities prevalent in cloudwater and aqueous aerosols. The main finding, however, is that hydroperoxides and α-hydroxyalkyl-hydroperoxides may not produce reactive free radicals by thermal[16,27−29] or photochemical O−O homolysis under atmospheric conditions.[30] Among organic peroxides, only diacyl peroxides could appreciably decompose into free radicals at ambient temperatures.[18,31]

EXPERIMENTAL SECTION

Figure S1 shows a schematic diagram of our experimental procedure for preparing α-HHs in solution.[24] Monoterpenes ($C_{10}H_{16}$, MW 136.13) or α-Tp ($C_{10}H_{16}OH$, MW 154.14) and NaCl were dissolved in 10 mL of W/AN mixtures (10, 20, 30, 40, 50, 60 vol % W for α-P, 20 and 50 vol % W for *d*-L, 20 and 50 vol % W for γ-Tn, and 50 and 100 vol % W for α-Tp) in a glass vial (25 mL). Note that the low solubilities of α-P (0.018 mM)[32] and other monoterpenes (except for α-Tp) preclude these studies in neat water. We use W/AN mixtures as surrogates of environmental aqueous SOA due to AN polarity and low reactivity toward O_3 and free radicals (SOA produced from the ozonolysis of α-pinene mainly consists of mixtures of polar hydrophilic species, such as dicarboxylic acids and esters, as well as some high-molecular-weight HOMs).[33] O_3 solutions were prepared separately by sparging 10 mL of the same W/AN mixtures in a 25 mL vial with O_3(g) from a commercial ozonizer (KSQ-050, Kotohira, Japan) fed with ultrahigh-purity O_2(g) (>99.999%). The ozonizer output gases were carried to the vial using Teflon tubing (3 mm i.d.) at 1 L/min flow rate (set by a digital mass flow controller) for 5−20 s. O_3 concentrations in the sparged solutions, [O_3(sol)], were determined by UV−vis spectroscopy (Agilent 8453) based on the reported O_3 molar extinction coefficient in the near-UV of $\varepsilon_{258\ nm}$ = 3840 M^{-1} cm^{-1} in water,[34] which is expected to be largely unaffected by the presence of AN.[35] Reactions were initiated by mixing terpene and ozone solutions (2.5 mL each) in a glass syringe (5 mL) covered with aluminum foil to avoid their photodegradation. To minimize unwanted secondary reactions, terpene concentrations were always in excess: $[\text{terpene}]_0/[O_3(\text{sol})]_0 > 15$. These mixtures were immediately injected (at 100 μL min^{-1} by a syringe pump, Harvard apparatus) into an ESI mass spectrometer (Agilent 6130 quadrupole LC/MS electrospray system at NIES, at Tsukuba). The pH of solutions was measured with a calibrated pH meter (LAQUA F-74, Horiba) before experiments. The evolution of α-HHs and other species was followed by ESI-MS as a function of time, recorded with a digital stopwatch.

The prominent feature of our experiments is that the presence of sub-millimolar NaCl allows us to detect by online ESI-MS and unambiguously establish the molecular masses of α-HHs and other multifunctional species (such as those containing −OOH, −OH, and −C═O groups) as chloride adducts without further manipulation.[7,36−42] We verified that the monofunctional *tert*-butyl hydroperoxide (TBHP), cumene hydroperoxide (CHP), as well as difunctional 1,6-hexanediol do not produce detectable Cl^- adducts in the presence of NaCl. The implication is that species should contain at least three functional groups to be detected as Cl^- adducts by ESI-MS. Chloride adducts characteristically appear as 3:1 doublets at m/z = M + 35 (+ 37) in the mass spectra.[7−10,43,44] We verified that Cl^- is inert toward O_3 ($k \approx 1 \times 10^{-2}$ M^{-1} s^{-1}) in the time scale of our experiments.[36]

The ESI mass spectrometer was operated as follows: nitrogen drying gas flow rate, 12 L min^{-1}; nitrogen drying gas temperature, 340 °C; inlet voltage, +3.5 kV relative to ground; fragmentor voltage, 60 V. All solutions were prepared in ultrapure water (resistivity ≥18.2 MΩ cm at 298 K) from a

https://dx.doi.org/10.1021/acs.est.9b07497
Environ. Sci. Technol. 2020, 54, 3890−3899

Millipore Milli-Q water purification system and used within a day. Chemicals (−)-α-pinene (≥95%, Wako or ≥99% Sigma-Aldrich), *d*-limonene (>99.0%, Tokyo Chemical Industry), γ-terpinene (>95.0%, Tokyo Chemical Industry), α-terpineol (>97.0%, Tokyo Chemical Industry), *tert*-butyl hydroperoxide (70 wt %, Sigma-Aldrich), cumene hydroperoxide (>80%, Tokyo Chemical Industry), 1,6-hexanediol (>97%, Tokyo Chemical Industry), acetonitrile (≥99.8%, Wako), tetrahydrofuran (≥99.8%, stabilizer free, Wako), D_2O (>99.9 atom % D, Sigma-Aldrich), $H_2{}^{18}O$ (≥97%, Cambridge Isotope Laboratories), NaCl (≥99.999%, Sigma-Aldrich), and HCl (37%, ACS reagent, Sigma-Aldrich) were used as received.

RESULTS AND DISCUSSION

Products of the Ozonolysis of α-Pinene in Water/Acetonitrile Mixtures. The products of the ozonolysis of α-P appear as negative ions in the online ESI mass spectra of (1 mM α-P + 0.2 mM NaCl + $[O_3]_0$ = 0.03 mM) solutions in W/AN (50:50 v/v; $[H_2O]$ = 27.8 M) mixtures (Figure 1).

O_3 should be consumed by excess α-P in a few milliseconds upon mixing 2.5 mL each of the (2 mM α-P + 0.4 mM NaCl) and 0.06 mM O_3 solutions. Our estimate is based on assuming that the reaction rate constants in the gas and liquid phases have similar values, i.e., $k(\alpha\text{-P} + O_3)_{liquid} \approx 6.0 \times 10^4\ M^{-1}\ s^{-1}$, from $k(\alpha\text{-P} + O_3)_{gas} = 1.0 \times 10^{-16}\ cm^3\ molecule^{-1}\ s^{-1}$.[45] Hence, O_3 would decay within $\tau_{1/e} \sim 17$ ms in [α-P] = 1 mM solutions. On the basis of previous studies,[46] we propose that O_3 adds to the α-P C=C double bond producing a primary ozonide,[7,47] which opens up into a stabilized CI (Scheme 2). The CI is expected to rapidly isomerize into a functionalized carboxylic acid (detected as a carboxylate, *m/z* 183) or competitively add water to produce a α-hydroxyalkyl-hydroperoxide (α-HH) (Scheme 2).[48]

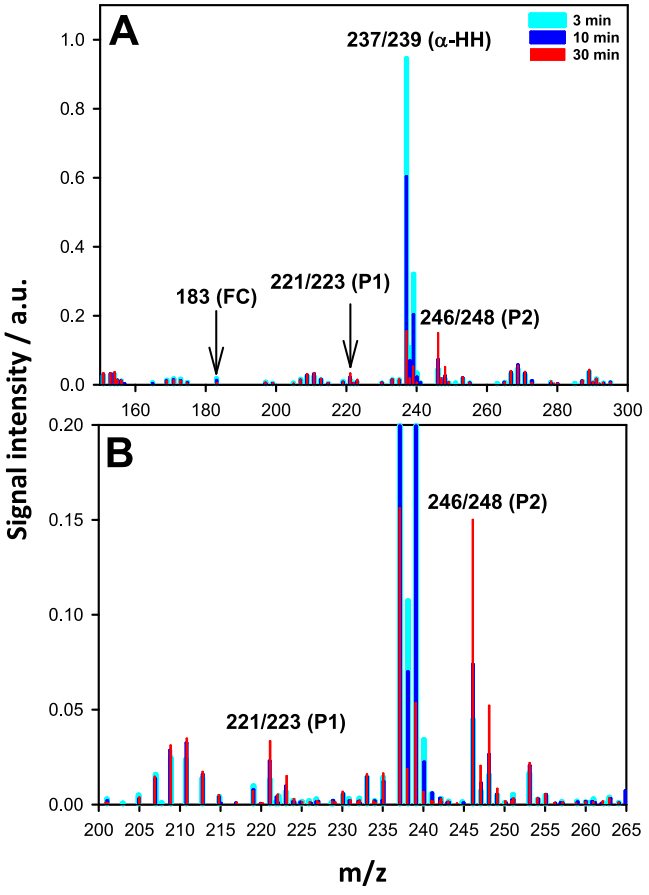

Figure 1. (A) Negative ion ESI mass spectra of (1 mM α-pinene + 0.2 mM NaCl + $[O_3]_0$ = 0.03 mM) in W/AN (50:50 by volume) at various times. (B) Zooming-in on slowly-generated products. P1 and P2 correspond to the chloride adducts of a *gem*-diol and a hydroperoxide-cyanohydrin, respectively. FC stands for functionalized carboxylate. See the text for details.

The intense peaks at *m/z* 237/239 are therefore assigned to the chloride adducts of the α-HH, 237/239 = 136 (α-P) + 48 (O_3) + 18 (H_2O) + 35/37 (Cl^-), in line with previous experiments from our laboratory.[44] The substitution of D_2O and $H_2{}^{18}O$ for $H_2{}^{16}O$ and the addition of an OH-radical scavenger support the assigned stoichiometries (see below). Establishing their molecular structures would require tandem mass spectrometric studies. The presence of chloride in the *m/z* 237/239 and other species is revealed by the characteristic 3-to-1 ratio of 237/239 signal intensities, which corresponds to the ratio of natural abundance $^{35}Cl/^{37}Cl$ chlorine isotopes. We also detect species at *m/z* 221/223 (P1) and 246/248 (P2) (see below) at longer reaction times (Figure 1B). Qualitatively similar results were obtained in the ozonolysis of the monoterpenes *d*-L and γ-Tn (see Figures S2−S6, Schemes S1 and S2). It should be emphasized that the absence of commercially available samples of α-HH and the products of its decomposition precluded determining their relative response factors and, hence, establishing mass balances from measured mass signal intensities.

We verified that the presence of 100 mM tetrahydrofuran (THF) (an efficient OH-radical scavenger, $k_{OH+THF} = 2.1 \times 10^9\ M^{-1}\ s^{-1}$)[49] in reaction mixtures has negligible effects on the extent of reaction or the products distribution: the same product signals appear at *m/z* 237/239 (α-HH), *m/z* 221/223 (P1), and 246/248 (P2) (Figure S7). This finding excludes the significant participation of OH-radicals in the formation or destruction of these species.[50]

Products of the Ozonolysis of α-Pinene in D_2O/Acetonitrile and $H_2{}^{18}O$/Acetonitrile Mixtures. The shifts of mass signals in D_2O/AN and $H_2{}^{18}O$/AN solutions are consistent with the proposed mechanism of α-HH formation (Scheme 2) and decomposition (Scheme 3). The fact that the *m/z* = 237/239 signals shift by +2 mass units to *m/z* 239/241 in both D_2O/AN and $H_2{}^{18}O$/AN (Figures S8 and S9) confirms the participation of one water molecule in the formation of the α-HH. A second water molecule substitutes an −O−H group for the −O−O−H functionality by eliminating H_2O_2 and producing an aldehyde whose *gem*-diol can exchange two O atoms via a keto ⇌ *gem*-diol equilibrium (Scheme 3). This is confirmed by the finding that the P1 (*m/z* 221/223) signals shift by +2 Da to *m/z* 223/225 in D_2O/AN (Figure S8) and by +4 Da to *m/z* 225/227 in $H_2{}^{18}O$/AN (Figure S9). We infer that α-HH decomposes by reacting with water via reaction R1:

$$\alpha\text{-HH} + 2H_2O \rightarrow \textit{gem}\text{-diol (P1)} + H_2O_2 \qquad \text{(R1)}$$

The P2 *m/z* 246/248 even-mass signals clearly correspond to a species containing one N atom. The molecular formula of P2 corresponds to the chloride adduct of the cyanohydrin resulting from the addition of HCN (an impurity from the partial hydrolysis of AN in W/AN mixtures) to an intermediate species derived from a fast CI isomerization channel:[51,52] *m/z* = 136 (α-P) + 48 (O_3) + 27 (HCN) + 35/37 (Cl^-) = 246/

https://dx.doi.org/10.1021/acs.est.9b07497
Environ. Sci. Technol. 2020, 54, 3890−3899

Scheme 2. Mechanism of α-Pinene Ozonolysis in Aqueous Phases[a]

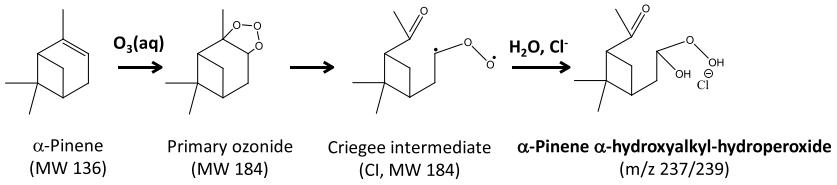

[a]Shown are what we consider the most likely structural isomers.

Scheme 3. Mechanism of α-Pinene α-Hydroxyalkyl-Hydroperoxide Reaction with Water[a]

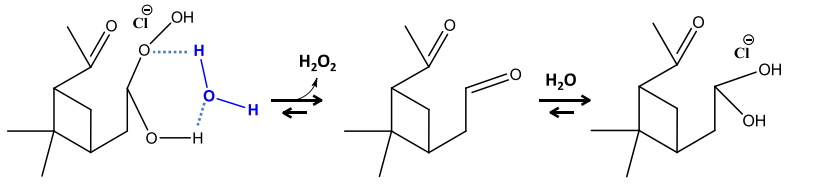

[a]Shown are what we consider the most likely among isomers.

248. We tentatively assign such intermediate to a vinyl-hydroperoxide (Scheme S3). The putative vinyl-hydroperoxide intermediate, by having a single −OOH group (such as TBHP and CHP, see above), is not expected to form a Cl^- adduct. The reasoning behind this assignment is that the delayed formation of P2 (see Figures 1B and 3) implies that HCN does not compete with water for the CI but, rather, reacts with a species simultaneously produced with the formation of the α-HH (Scheme S3). A P2 cyanohydrin containing −OH and −OOH groups that can exchange protons for deuterons accounts for the +2 Da shifts undergone by the 246/248 signals in D_2O/AN (Figure S8). The +2 Da shifts in $H_2{}^{18}O$/AN mixtures are tentatively ascribed to O atom exchange between $H_2{}^{18}O$ and the carbonyl O atom of the vinyl-hydroperoxide (Figure S9). We note that HCN does not add to the carbonyl group of the α-HH (a reaction that would have produced a species appearing at m/z 264/268), possibly because the carbonyl is blocked by intramolecular hydrogen bonding with the −C(−OH)(−OOH) group.

Products of the Ozonolysis of α-Terpineol in Water and Water/Acetonitrile Mixtures. Negative ion mass spectra as functions of time in the ozonolysis of (α-Tp + NaCl) in 100% W and W/AN (50:50) mixtures are shown in Figure 2. The intense peaks at m/z 255/257 are ascribed to the chloride adducts of the α-Tp α-HH, 255/257 = 154 (α-Tp) + 48 (O_3) + 18 (H_2O) + 35/37 (Cl^-) (Scheme 4), in line with results for the ozonolysis of α-Tp at the air−water interface.[53] The presence of a hydroperoxide-cyanohydrin, detected as a chloride adduct at m/z = 264/266 = 154 (α-Tp) + 48 (O_3) + 27 (HCN) + 35/37 (Cl^-), in W/AN (50:50) (Figure 2B), and its absence in pure W (Figure 2A), confirms that HCN originates from the partial hydrolysis of AN in W/AN mixtures.

Kinetic Experiments. The temporal profiles of the detected products of α-P ozonolysis, namely, the α-HH (m/z 237/239), P1 (m/z 221/223), and P2 (m/z 246/248), in W/AN (50:50, [W] = 27.8 M and 20:80, [W] = 11.1 M) are shown in Figure 3, parts A and B. In both mixtures, α-HH (m/z 237/239) signals decay as single exponentials (see below)

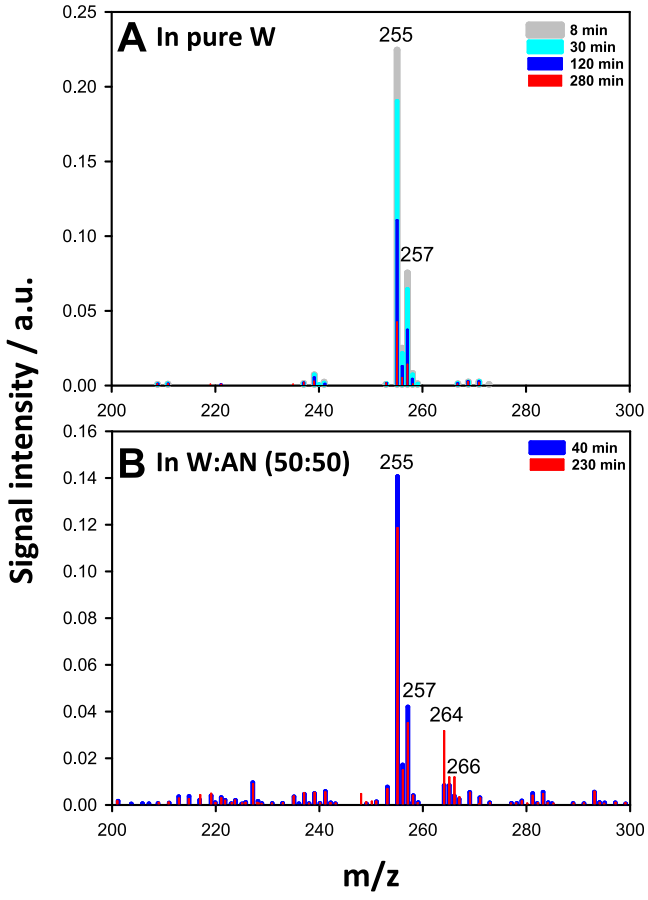

Figure 2. (A) Negative ion mass spectra of 1 mM α-terpineol + 0.2 mM NaCl + $[O_3]_0 \approx 0.04$ mM in neat water and (B) in a W/AN (50:50) mixture, at various times.

with rate coefficients of k_1(20:80) = (2.7 ± 1.7) × 10^{-4} s^{-1} and k_1(50:50) = (1.1 ± 0.1) × 10^{-3} s^{-1}, the averages of four independent runs. These k_1 values correspond to $\tau_{1/e}$ = 62 and 15 min, respectively. The rate coefficients determined in the

https://dx.doi.org/10.1021/acs.est.9b07497
Environ. Sci. Technol. 2020, 54, 3890−3899

Scheme 4. Mechanism of the Ozonolysis of α-Terpineol in Water/Acetonitrile[a]

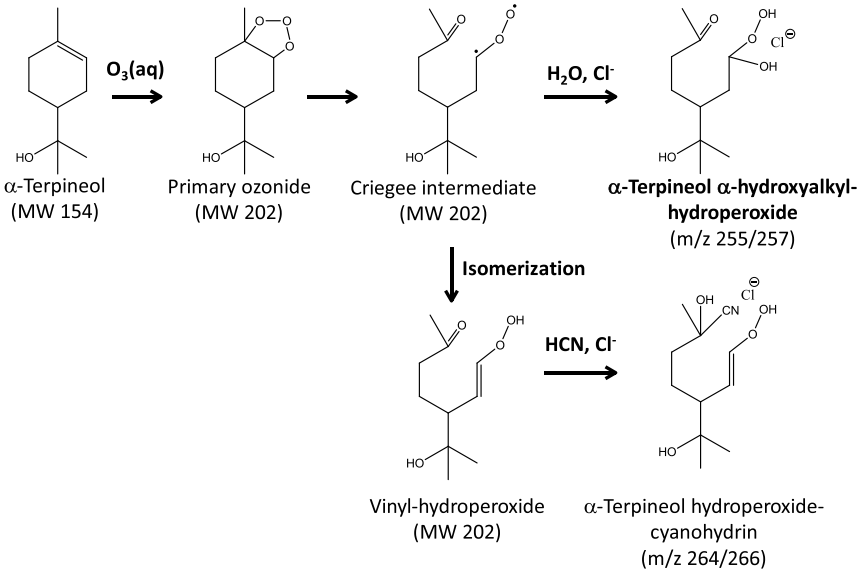

[a]Shown are what we consider the most likely among isomers.

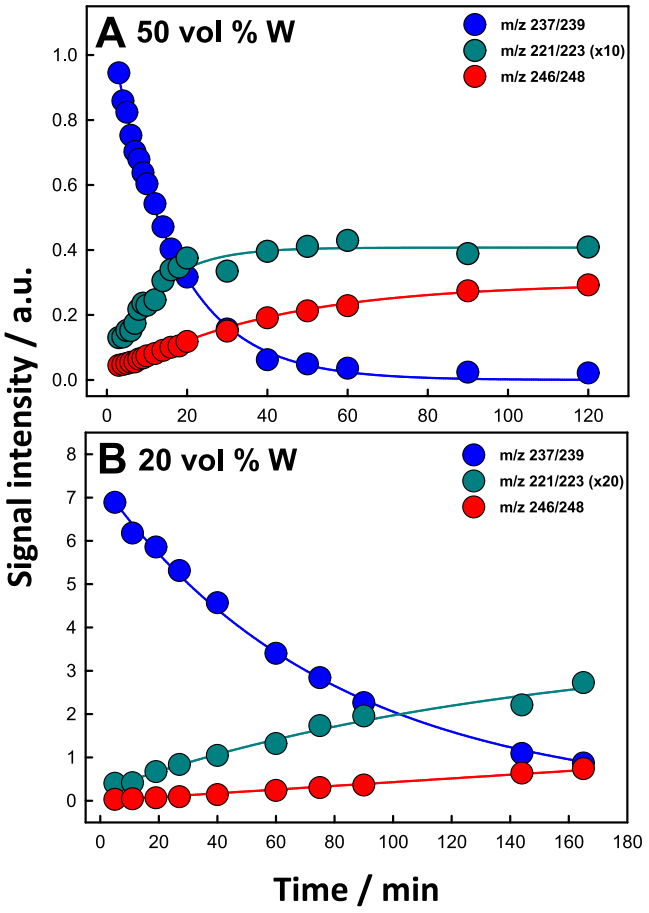

Figure 3. Temporal profiles of the chloride adducts of the products of α-pinene ozonolysis of (1 mM α-pinene, 1 mM NaCl, $[O_3]_0$ = 0.05 mM) in (A) 50:50 and (B) 20:80 W/AN mixtures: blue, α-HH (*m*/*z* 237/239); dark cyan, P1 (*m*/*z* 221/223); red, P2 (*m*/*z* 246/248). P1 signal intensities were multiplied by 10 (A) and 20 (B), respectively. Lines correspond to fitting signal intensities (*S*) vs time with $S = S_0 \exp(-k_1 t)$ or $S = S_{max}[1 - \exp(-kt)]$ functions. See text for details.

present study are summarized in Table 1. In similar experiments, we had found that the α-HH from the ozonolysis

Table 1. Rate Coefficients of α-HHs Decay in Water/Acetonitrile Mixtures vs Water Vol % at 298 ± 3 K

terpene	water (vol %)	k (10^{-4} s^{-1})[a]	$\tau_{1/e}$ (min)
α-pinene	10	0.26 ± 0.11*	641
	20	2.7 ± 1.7	62
	30	3.2 ± 1.5	52
	40	6.1 ± 0.6	27
	50	11 ± 1	15
	60	12 ± 2	14
d-limonene	20	1.3 ± 1.0*	128
	50	12 ± 3	14
γ-terpinene	20	0.48 ± 0.29	347
	50	3.7 ± 1.5	45
α-terpineol	50	0.16 ± 0.01	1042
	100	1.3 ± 0.4	128
	100[b]	1.0 ± 0.1	167
β-caryophyllene[c]	10	0.031 ± 0.002*	5376
	20	1.4 ± 0.6	119
	30	1.4 ± 0.2	119
	40	1.7 ± 0.4	98
	50	3.2 ± 0.7	52

[a]Rate coefficients are k_1 values derived from experimental α-HH signal intensity (*S*) fits by single-exponential decay functions, $S = S_{01} \exp(-k_1 t)$, ($\tau_{1/e} = 1/k_1$), except those marked with an asterisk (*), which correspond to k_2 for the slower component of the observed biexponential decays, $S = S_{01} \exp(-k_1 t) + S_{02} \exp(-k_2 t)$ ($\tau_{1/e} = 1/k_2$). [b]In the presence of 1 μM $FeCl_2$. [c]From ref 25. See text for details.

of β-caryophyllene in 50:50 mixtures decayed in $\tau_{1/e}$ = 52 min.[25] Inspection of the data in Table 1 and Figure 4 shows that the decay of α-P α-HH becomes significantly slower in solvent mixtures of lower water content. The dependence of k_1 on water content, however, is not linear as would be expected from the fact that water is a reactant in reaction R1. Remarkably, while $\tau_{1/e}$ = 52 min in 30% water slightly increases to $\tau_{1/e}$ = 62 min in 20% water, the decay of α-HH in

https://dx.doi.org/10.1021/acs.est.9b07497
Environ. Sci. Technol. 2020, 54, 3890−3899

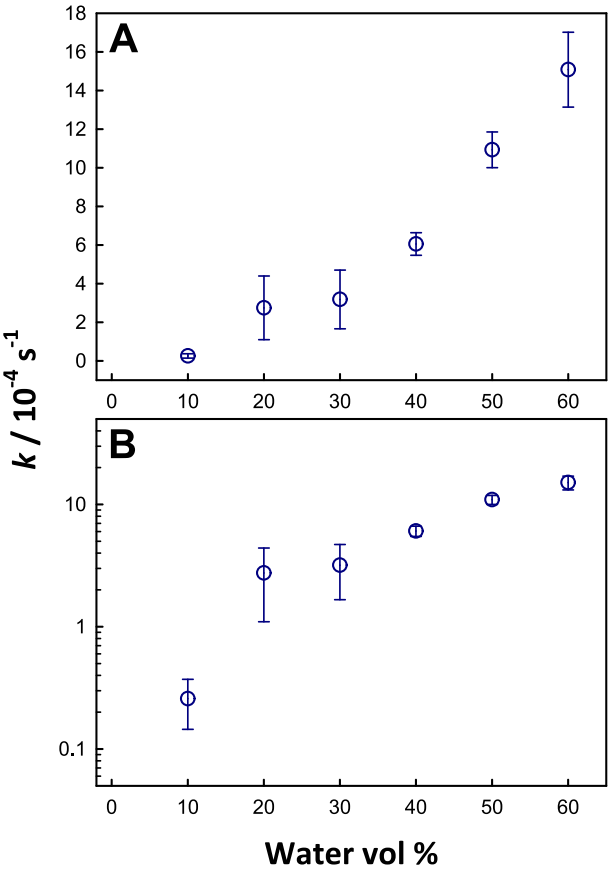

Figure 4. (A) First-order rate coefficients k_1 of the decay of the chloride adduct of α-pinene α-HH (m/z 237/239) in W/AN mixtures as a function of water volume, at 298 ± 3 K. Data are from Table 1. k_1 values were derived by fitting α-HH signal intensities (S) vs time with $S = S_0 \exp(-k_1 t)$, except in the case of the 10% W mixture where the plotted value is k_2 from $S = S_{01} \exp(-k_1 t) + S_{02} \exp(-k_2 t)$ fits. See text for details. Error bars are derived from three to four independent measurements. (B) The semilog plot shows the dramatic increase of α-HH persistence in 10% W.

10% water is dramatically different. In the 10% water mixture, α-HH decays by ∼35% in the first 15 min followed by a much slower decay that extends for hours (Figure S11).

It should be realized that if water molecules were homogeneously mixed at the molecular level the decay of α-HH would be a single-exponential function because water participates as a reagent in both the consecutive reactions in Scheme 3. The decay of α-HH signal intensities (S) in 10:90 mixtures is well-represented by a biexponential function $S = S_{01} \exp(-k_1 t) + S_{02} \exp(-k_2 t)$ (Figure S11), with $\tau_{1/e} = 1/k_2 = 641$ min (Table 1). The observed fast and slow regimes are indicative of the availability of water to α-HHs in W/AN water-rich and water-poor domains of molecular dimensions (see below). The α-HHs from d-L and β-caryophyllene display a similar behavior in 20:80 and 10:90 mixtures.[25]

We also analyzed the rise of product signal intensities with time. The evolution of P1 (m/z 221/223) signal intensities with time (Figure 3) in α-P experiments is well-fitted by $S = S_{max}[1 - \exp(-k_{P1} t)]$ functions. Four independent measurements led to $k_{P1} = (1.6 \pm 0.2) \times 10^{-3}$ s^{-1} in 50:50 mixtures and $k_{P1} = (2.0 \pm 0.2) \times 10^{-4}$ s^{-1} in 20:80 mixtures. These values compare well with the $k_1 = (1.1 \pm 0.1) \times 10^{-3}$ and $(2.7 \pm 1.7) \times 10^{-4}$ s^{-1} values for α-HH decays in the same mixtures, confirming that P1 is a direct product of α-HH decomposition. On the basis of this result and the P1 mass shifts in D_2O/AN and $H_2{}^{18}O$/AN experiments, we assign P1 to the [1-(3-(2,2-dihydroxyethyl)-2,2-dimethylcyclobutyl)-ethenone] *gem*-diol produced from the substitution of an −OH for the −OOH group in α-HH (Scheme 3). Because α-HH signals decay to zero in all cases, except in 10% water, the equilibrium, α-HH = P1 + H_2O_2, is fully shifted to the products side (Scheme 3).[54] In contrast, the rise P2 (m/z 246/248) signal intensities in 50:50 mixtures, $S = S_{max}[1 - \exp(-k_{P2} t)]$, corresponds to $k_{P2} = (4.2 \pm 0.3) \times 10^{-4}$ s^{-1}. This value is about 4 times smaller than k_1 indicating that P2 is not a product of α-HH decomposition (Scheme 4).

To recapitulate, the data of Table 1 reveal that in 50:50 mixtures the α-HHs from α-P and d-L decompose into H_2O_2 at comparable rates, which are ∼3 times faster than the α-HH from γ-Tn and ∼70 times faster than that from α-Tp. Decay rates markedly increase in a nonlinear manner with water content. The α-HH from α-P, the most abundant biogenic monoterpene in the atmosphere, lasts from tens of minutes in >20% water mixtures to ∼9 h in ≤10% water. Below we show that the rapid conversion of α-HHs to H_2O_2 in SOA under atmospheric conditions may preempt their decomposition into free radicals via solar photolysis[22,55] or via catalysis by transition metal ions.[29,30]

We analyze the physicochemical underpinnings of these findings and their potential implications for the fate and quantification of hydroperoxides in SOA. In the case of α-P, the strong nonlinear dependence on water content of the rate constants (k_1 or k_2, see above) for the α-HH + H_2O reaction (Figure 4) implies that H_2O is not directly accessible to the α-HH in these solvent mixtures. We had observed a similar nonlinear behavior in the decay of the α-HH produced from the ozonolysis of β-caryophyllene.[25,56] We propose that this is evidence that α-HHs are produced in discrete domains where water accessibility depends on their structure and water exchange dynamics, rather than in molecularly homogeneous media.

These domains are generally present in mixtures of water with miscible organic solvents.[57−59] This is substantiated by small-angle neutron and dynamic light scattering experiments that detect short-lived (<50 ps), short-ranged (∼1 nm) concentration fluctuations in most water−hydrotrope mixtures[58−60] and with recent reactivity and selectivity studies in these media.[57,59] A recent soft X-ray absorption spectroscopic study of W/AN mixtures presented evidence of micro-heterogeneity.[61] Ab initio quantum chemical inner-shell calculations suggested that the three distinct regions observed in these mixtures result from the interplay of hydrogen bonding and dipolar interactions between water and acetonitrile molecules.[61] Notably, the discontinuity observed at ≈13 vol % W (molar fraction of water $x_w = 0.3$) was ascribed to a transition between phases mainly containing AN-rich large W_nAN_m clusters below $x_w = 0.3$ and smaller clusters held by dipolar interactions above $x_w = 0.3$.[61] We believe that the dramatic increase of α-HH persistence below 20 vol % W is associated with such phase transition. Additional evidence is provided by the nonlinear dependences of the intensity, peak emission wavelength, and decay lifetime of 7-cyanoindole fluorescence in W/AN and other eight W−hydrotope mixtures as functions of water molar fraction.[62] The fact that 7-cyanoindole fluorescence in W/AN decayed as a single exponential in the 2−12 ns range indicated that 7-cyanoindole

https://dx.doi.org/10.1021/acs.est.9b07497
Environ. Sci. Technol. 2020, 54, 3890−3899

fluoresced while embedded in the most abundant W_nAN_m clusters of the (n, m) distribution.

Against this backdrop, our results suggest that α-HHs (reaction R1) are generated in situ from the ozonolysis of monoterpenes embedded in W_nAN_m clusters rather than dissolved in molecularly homogeneous solutions. The accessibility of H_2O to α-HHs should depend on the composition and rearrangement dynamics of W_nAN_m clusters rather than on the macroscopic concentration of water. In such scenario, the limited rapid initial decay of α-HHs followed by a much slower process in 10:90 mixtures may reflect the (n, m) distribution of W_nAN_m clusters. In 10:90 mixtures, only a few clusters would contain a significant number of water molecules, those accounting for the fast α-HH decay. Since microheterogeneity should be a general phenomenon in "internally mixed" aqueous organic mixtures, we suggest that the existence of inhomogeneities at the molecular level, as distinct from mesoscopic segregation,[63−65] could play unanticipated roles in atmospheric aqueous media.[56]

The relatively short lifetimes of the α-HHs derived from the ozonolysis of monoterpenes relative to the dramatic persistence of the α-HH derived from α-Tp (Table 1 and Figure S12) are another unanticipated outcome, because it is difficult to envision a long-range intramolecular effect (through four bonds) of the −OH group on the reactivity of the R−(H)C(−OH)(−OOH) group. Even in pure W, the α-Tp-derived α-HH survives for over 2 h. One possibility is that water molecules bridge −OH and −OOH groups via extended hydrogen bonding, thereby blocking the formation of the six-membered transition state for the α-HH decomposition into aldehyde + H_2O_2 (Scheme 1). Another possibility involves an orientation effect whereby the polar exo −OH group of α-Tp forces the hydrophobic backbone containing the endo C═C bond (and, as a result, the R−(H)C(−OOH)(−OH) group) to AN-rich cluster cores in W/AN mixtures.[61]

pH Effects on the Decay Rates of α-Tp-derived α-HH in Pure Water. Finally, we investigated the pH dependence (in the pH = 2.3−3.3 range, adjusted by HCl additions) on the kinetics of decomposition of α-Tp-derived α-HH in pure water. The results are shown in Table 2.

Table 2. Rate Coefficients of α-Tp-Derived α-HHs Decay in Water vs pH at $[\alpha\text{-Tp}]_0$ = 1 mM, $[O_3]_0$ = 0.06 mM at 298 ± 3 K

α-terpineol		
pH	K_1 (10^{-4} s^{-1})	$\tau_{1/e}$ (min)[a]
2.3	8.7 ± 1.0	19
2.6	4.4 ± 0.5	38
3.0	3.0 ± 0.2	56
3.3	2.5 ± 0.2	66
6.1 (as is)	1.3 ± 0.4	128

[a] $\tau_{1/e} = 1/k_1$.

It is apparent that decomposition rates are accelerated at lower pH, implying an acid-catalyzed reaction. This is an important effect, considering that ambient cloudwater and aqueous aerosols are more acidic than previously assumed.[66−68] This finding is in contrast with the opposite pH effect reported for the decomposition of α-acyloxyalkyl-hydroperoxides, produced from α-P's CIs reactions with pinonic and adipic acids.[40] Zhao et al. reported the linear increase in the first-order decay rate coefficient as pH increased from 3.5 to 5.1, which is consistent with an OH^- catalyzed decomposition.[40] The different behaviors may be ascribed to the key role played by the α-OH group in R(−H)(−OH)-(−OOH) decomposition, which is absent in α-acyloxyalkyl-hydroperoxides R(−H)(−OR′)(−OOH).

Atmospheric Implications. The fast decomposition of monoterpene-derived α-HHs, e.g., $\tau_{1/e}$ ∼ 15 min in 50 vol % water, suggests that significant losses may occur prior to off-line chemical analyses of SOA samples whether collected in the field or synthesized in the laboratory.[39,40,69] We suggest that discordant results obtained under otherwise similar conditions could be due to variations, depending on relative humidity or water content, to the nonlinear dependence of k_1 on water content and to the onset of the much slower component of biexponential decays in <20% water media.

Regarding the role of α-HHs in SOA aging, our findings reveal that their decomposition does not yield free radicals but H_2O_2 via reaction R1. Reaction R1 however preserves the peroxide content and, therefore, the potential toxicity of SOA.[50,70,71] Regarding the putative role of free radicals in SOA aging from the decomposition of RC−OOH hydroperoxides, we point out that thermal decomposition studies in dilute solutions show that the homolysis of RO−OH bonds proceeds with $\tau_{1/2}$ = 10 h half-lives at temperatures above 130 °C.[18] In other words, neither RC−OOH hydroperoxides nor R−(H)C(−OH)(−OOH) α-hydroxyalkyl-hydroperoxides could conceivably produce free radicals in SOA at ambient temperatures. On the other hand, UV−vis spectra of 1 mM β-caryophyllene in W/AN (50:50) before and after ozonolysis (Figure S13) show that the peak absorption of reaction products occurs at ∼280 nm, which corresponds to carbonyl chromophores. Thus, the solar photolysis of α-HHs and their products will be dominated by carbonyl rather than peroxide photochemistry.[22,72]

Fenton-like chemistry is expected to take place in hours rather than in tens of minutes under typical conditions.[22,55] From representative values of $[Fe^{2+}] \sim 10^{-7}$ M, [ROOH] ∼ 10^{-6} M in aqueous aerosol/cloud droplets,[30,54] and $k(Fe^{2+}$ + ROOH) ∼ 20 M^{-1} s^{-1},[29] we estimate $\tau_{1/e}$ > 14 h for Fenton-like α-HHs decompositions, which is much longer than the $\tau_{1/e}$ < 1 h values derived from the data of Table 1. We confirmed the slowness of Fenton-like chemistry in the time frame of our experiments by showing that the presence of catalytic concentrations of Fe^{2+} did not even accelerate the slow decay of the α-HH derived from the ozonolysis of (1 mM α-Tp + 0.2 mM NaCl + 1 μM $FeCl_2$) in neat water (Table 1).

In summary, we found that the α-HHs derived from the ozonolysis of atmospherically important monoterpenes react with water to produce *gem*-diols + H_2O_2 rather than free radicals. α-HHs decay mono- or biexponentially depending on both molecular structure and solvent composition. $\tau_{1/e}$'s in water-rich solvent mixtures range from $\tau_{1/e}$ = 15−45 min for monoterpene-derived α-HHs to $\tau_{1/e}$ > 10^3 min for the α-Tp-derived α-HH. Remarkably, all $\tau_{1/e}$'s dramatically increase in <20% (v/v) water. The decomposition of the α-Tp-derived α-HH in pure water is accelerated at lower pH in the pH 2.3−3.3 range. The residual hydroperoxides detected in day-old SOA samples may reflect the slower components of biexponential decays in water-poor media and/or the slow decomposition of α-HHs from functionalized terpenes.

https://dx.doi.org/10.1021/acs.est.9b07497
Environ. Sci. Technol. 2020, 54, 3890−3899

■ ASSOCIATED CONTENT

Supporting Information

The Supporting Information is available free of charge at https://pubs.acs.org/doi/10.1021/acs.est.9b07497.

Additional experimental data, including the schematic setup and procedure, mass spectra, temporal profiles, UV−vis spectra, and mechanism schemes (PDF)

■ AUTHOR INFORMATION

Corresponding Authors

Agustín J. Colussi − *Ronald and Maxine Linde Center for Global Environmental Science, California Institute of Technology, Pasadena, California 91125, United States;* orcid.org/0000-0002-3400-4101; Phone: +1-626-396-6350; Email: ajcoluss@caltech.edu

Shinichi Enami − *National Institute for Environmental Studies, Tsukuba 305-8506, Japan;* orcid.org/0000-0002-2790-7361; Phone: +81-29-850-2770; Email: enami.shinichi@nies.go.jp

Authors

Junting Qiu − *Graduate School of Frontier Sciences, The University of Tokyo, Kashiwa 277-8563, Japan*

Zhancong Liang − *School of Atmospheric Sciences, Sun Yat-sen University, Guangzhou 510275, China*

Kenichi Tonokura − *Graduate School of Frontier Sciences, The University of Tokyo, Kashiwa 277-8563, Japan;* orcid.org/0000-0003-1910-8508

Complete contact information is available at: https://pubs.acs.org/10.1021/acs.est.9b07497

Author Contributions

S.E. designed research, J.Q., Z.L., and S.E. performed experiments, and S.E. contributed new reagents/analytical tools. All authors analyzed data and wrote the paper.

Notes

The authors declare no competing financial interest.

■ ACKNOWLEDGMENTS

S.E. is grateful to the JSPS KAKENHI Grant No. 19H01154. A.J.C. acknowledges support from the National Science Foundation U.S.A., Grant AGS-1744353.

■ REFERENCES

(1) Ehn, M.; Thornton, J. A.; Kleist, E.; Sipila, M.; Junninen, H.; Pullinen, I.; Springer, M.; Rubach, F.; Tillmann, R.; Lee, B.; et al. A large source of low-volatility secondary organic aerosol. *Nature* **2014**, *506* (7489), 476−479.

(2) Jokinen, T.; Berndt, T.; Makkonen, R.; Kerminen, V.-M.; Junninen, H.; Paasonen, P.; Stratmann, F.; Herrmann, H.; Guenther, A. B.; Worsnop, D. R.; et al. Production of extremely low volatile organic compounds from biogenic emissions: Measured yields and atmospheric implications. *Proc. Natl. Acad. Sci. U. S. A.* **2015**, *112* (23), 7123−7128.

(3) Tröstl, J.; Chuang, W. K.; Gordon, H.; Heinritzi, M.; Yan, C.; Molteni, U.; Ahlm, L.; Frege, C.; Bianchi, F.; Wagner, R.; et al. The role of low-volatility organic compounds in initial particle growth in the atmosphere. *Nature* **2016**, *533* (7604), 527.

(4) Shrivastava, M.; Cappa, C. D.; Fan, J.; Goldstein, A. H.; Guenther, A. B.; Jimenez, J. L.; Kuang, C.; Laskin, A.; Martin, S. T.; Ng, N. L.; et al. Recent advances in understanding secondary organic aerosol: Implications for global climate forcing. *Rev. Geophys.* **2017**, *55* (2), 509−559.

(5) Spracklen, D.; Jimenez, J.; Carslaw, K.; Worsnop, D.; Evans, M.; Mann, G.; Zhang, Q.; Canagaratna, M.; Allan, J.; Coe, H.; et al. Aerosol mass spectrometer constraint on the global secondary organic aerosol budget. *Atmos. Chem. Phys.* **2011**, *11* (23), 12109−12136.

(6) Gong, Y.; Chen, Z.; Li, H. The oxidation regime and SOA composition in limonene ozonolysis: roles of different double bonds, radicals, and water. *Atmos. Chem. Phys.* **2018**, *18* (20), 15105−15123.

(7) Enami, S.; Colussi, A. J. Criegee Chemistry on Aqueous Organic Surfaces. *J. Phys. Chem. Lett.* **2017**, *8*, 1615−1623.

(8) Enami, S.; Colussi, A. J. Efficient scavenging of Criegee intermediates on water by surface-active cis-pinonic acid. *Phys. Chem. Chem. Phys.* **2017**, *19*, 17044−17051.

(9) Enami, S.; Colussi, A. J. Reactions of Criegee Intermediates with Alcohols at Air-Aqueous Interfaces. *J. Phys. Chem. A* **2017**, *121*, 5175−5182.

(10) Enami, S.; Hoffmann, M. R.; Colussi, A. J. Criegee Intermediates React with Levoglucosan on Water. *J. Phys. Chem. Lett.* **2017**, *8* (16), 3888−3894.

(11) Praske, E.; Otkjaer, R. V.; Crounse, J. D.; Hethcox, J. C.; Stoltz, B. M.; Kjaergaard, H. G.; Wennberg, P. O. Atmospheric autoxidation is increasingly important in urban and suburban North America. *Proc. Natl. Acad. Sci. U. S. A.* **2018**, *115* (1), 64−69.

(12) Praske, E.; Otkjaer, R. V.; Crounse, J. D.; Hethcox, J. C.; Stoltz, B. M.; Kjaergaard, H. G.; Wennberg, P. O. Intramolecular Hydrogen Shift Chemistry of Hydroperoxy-Substituted Peroxy Radicals. *J. Phys. Chem. A* **2019**, *123* (2), 590−600.

(13) Bianchi, F.; Kurtén, T.; Riva, M.; Mohr, C.; Rissanen, M. P.; Roldin, P.; Berndt, T.; Crounse, J. D.; Wennberg, P. O.; Mentel, T. F.; et al. Highly Oxygenated Organic Molecules (HOM) from Gas-Phase Autoxidation Involving Peroxy Radicals: A Key Contributor to Atmospheric Aerosol. *Chem. Rev.* **2019**, *119* (6), 3472−3509.

(14) Claflin, M. S.; Krechmer, J. E.; Hu, W.; Jimenez, J. L.; Ziemann, P. J. Functional group composition of secondary organic aerosol formed from ozonolysis of α-pinene under high VOC and autoxidation conditions. *ACS Earth Space Chem.* **2018**, *2* (11), 1196−1210.

(15) Zhang, X.; Lambe, A. T.; Upshur, M. A.; Brooks, W. A.; Gray Bé, A.; Thomson, R. J.; Geiger, F. M.; Surratt, J. D.; Zhang, Z.; Gold, A.; et al. Highly oxygenated multifunctional compounds in α-pinene secondary organic aerosol. *Environ. Sci. Technol.* **2017**, *51* (11), 5932−5940.

(16) Hiatt, R.; Mill, T.; Mayo, F. R. Homolytic decompositions of hydroperoxides.i. Summary and implications for autoxidation. *J. Org. Chem.* **1968**, *33* (4), 1416−1420.

(17) Kharasch, M.; Fono, A.; Nudenberg, W. The chemistry of hydroperoxides. III. The free-radical decomposition of hydroperoxides. *J. Org. Chem.* **1950**, *15* (4), 763−774.

(18) Sanchez, J.; Myers, T. N. Peroxides and peroxide compounds, organic peroxides. In *Kirk-Othmer Encyclopedia of Chemical Technology*; John Wiley and Sons: Hoboken, NJ, 2000.

(19) Tong, H.; Zhang, Y.; Filippi, A.; Wang, T.; Li, C.; Liu, F.; Leppla, D.; Kourtchev, I.; Wang, K.; Keskinen, H.-M.; et al. Radical Formation by Fine Particulate Matter Associated with Highly Oxygenated Molecules. *Environ. Sci. Technol.* **2019**, *53*, 12506.

(20) Tong, H. J.; Arangio, A. M.; Lakey, P. S. J.; Berkemeier, T.; Liu, F. B.; Kampf, C. J.; Brune, W. H.; Poschl, U.; Shiraiwa, M. Hydroxyl radicals from secondary organic aerosol decomposition in water. *Atmos. Chem. Phys.* **2016**, *16* (3), 1761−1771.

(21) Mertes, P.; Pfaffenberger, L.; Dommen, J.; Kalberer, M.; Baltensperger, U. Development of a sensitive long path absorption photometer to quantify peroxides in aerosol particles (Peroxide-LOPAP). *Atmos. Meas. Tech.* **2012**, *5* (10), 2339−2348.

(22) Krapf, M.; El Haddad, I.; Bruns, E. A.; Molteni, U.; Daellenbach, K. R.; Prévôt, A. S.; Baltensperger, U.; Dommen, J. Labile peroxides in secondary organic aerosol. *Chem.* **2016**, *1* (4), 603−616.

(23) Fuller, S.; Wragg, F.; Nutter, J.; Kalberer, M. Comparison of on-line and off-line methods to quantify reactive oxygen species (ROS) in atmospheric aerosols. *Atmos. Environ.* **2014**, *92*, 97−103.

(24) Qiu, J.; Ishizuka, S.; Tonokura, K.; Enami, S. Interfacial vs Bulk Ozonolysis of Nerolidol. *Environ. Sci. Technol.* **2019**, *53*, 5750−5757.
(25) Qiu, J.; Ishizuka, S.; Tonokura, K.; Colussi, A. J.; Enami, S. Water Dramatically Accelerates the Decomposition of alpha-Hydroxyalkyl-Hydroperoxides in Aerosol Particles. *J. Phys. Chem. Lett.* **2019**, *10*, 5748−5755.
(26) Guenther, A. B.; Jiang, X.; Heald, C. L.; Sakulyanontvittaya, T.; Duhl, T.; Emmons, L. K.; Wang, X. The Model of Emissions of Gases and Aerosols from Nature version 2.1 (MEGAN2.1): an extended and updated framework for modeling biogenic emissions. *Geosci. Model Dev.* **2012**, *5* (6), 1471−1492.
(27) Hiatt, R. R.; Mill, T.; Irwin, K. C.; Castleman, J. K. Homolytic decompositions of hydroperoxides. II. Radical-induced decompositions of tert-butyl hydroperoxide. *J. Org. Chem.* **1968**, *33* (4), 1421−1428.
(28) Zhao, R.; Lee, A.; Soong, R.; Simpson, A.; Abbatt, J. Formation of aqueous-phase α-hydroxyhydroperoxides (α-HHP): potential atmospheric impacts. *Atmos. Chem. Phys.* **2013**, *13* (12), 5857−5872.
(29) Chevallier, E.; Jolibois, R. D.; Meunier, N.; Carlier, P.; Monod, A. "Fenton-like" reactions of methylhydroperoxide and ethylhydroperoxide with Fe^{2+} in liquid aerosols under tropospheric conditions. *Atmos. Environ.* **2004**, *38* (6), 921−933.
(30) Deguillaume, L.; Leriche, M.; Chaumerliac, N. Impact of radical versus non-radical pathway in the Fenton chemistry on the iron redox cycle in clouds. *Chemosphere* **2005**, *60* (5), 718−724.
(31) Leffler, J.; More, A. Decomposition of bicyclo [2.2. 2]-1-formyl and pivaloyl peroxides. *J. Am. Chem. Soc.* **1972**, *94* (7), 2483−2487.
(32) Li, J.; Perdue, E. M.; Pavlostathis, S. G.; Araujo, R. Physicochemical properties of selected monoterpenes. *Environ. Int.* **1998**, *24* (3), 353−358.
(33) Zhang, X.; McVay, R. C.; Huang, D. D.; Dalleska, N. F.; Aumont, B.; Flagan, R. C.; Seinfeld, J. H. Formation and evolution of molecular products in α-pinene secondary organic aerosol. *Proc. Natl. Acad. Sci. U. S. A.* **2015**, *112* (46), 14168−14173.
(34) Ferre-Aracil, J.; Cardona, S. C.; Navarro-Laboulais, J. Determination and Validation of Henry's Constant for Ozone in Phosphate Buffers Using Different Analytical Methodologies. *Ozone: Sci. Eng.* **2015**, *37* (2), 106−118.
(35) Ershov, B. G.; Panich, N. M. Spectrophotometric determination of ozone in solutions: Molar absorption coefficient in the visible region. *Spectrochim. Acta, Part A* **2019**, *217*, 39−43.
(36) Hoigne, J.; Bader, H.; Haag, W. R.; Staehelin, J. Rate constants of reactions of ozone with organic and inorganic-compounds in water. III. inorganic-compounds and radicals. *Water Res.* **1985**, *19* (8), 993−1004.
(37) Enami, S.; Vecitis, C. D.; Cheng, J.; Hoffmann, M. R.; Colussi, A. J. Global inorganic source of atmospheric bromine. *J. Phys. Chem. A* **2007**, *111* (36), 8749−8752.
(38) Zhou, S. M.; Rivera-Rios, J. C.; Keutsch, F. N.; Abbatt, J. P. D. Identification of organic hydroperoxides and peroxy acids using atmospheric pressure chemical ionization-tandem mass spectrometry (APCI-MS/MS): application to secondary organic aerosol. *Atmos. Meas. Tech.* **2018**, *11* (5), 3081−3089.
(39) Zhao, R.; Kenseth, C. M.; Huang, Y.; Dalleska, N. F.; Seinfeld, J. H. Iodometry-Assisted Liquid Chromatography Electrospray Ionization Mass Spectrometry for Analysis of Organic Peroxides: An Application to Atmospheric Secondary Organic Aerosol. *Environ. Sci. Technol.* **2018**, *52* (4), 2108−2117.
(40) Zhao, R.; Kenseth, C. M.; Huang, Y.; Dalleska, N. F.; Kuang, X. M.; Chen, J.; Paulson, S. E.; Seinfeld, J. H. Rapid Aqueous-Phase Hydrolysis of Ester Hydroperoxides Arising from Criegee Intermediates and Organic Acids. *J. Phys. Chem. A* **2018**, *122*, 5190−5201.
(41) Allen, H. M.; Crounse, J. D.; Bates, K. H.; Teng, A. P.; Krawiec-Thayer, M. P.; Rivera-Rios, J. C.; Keutsch, F. N.; St. Clair, J. M.; Hanisco, T. F.; Møller, K. H.; et al. Kinetics and Product Yields of the OH Initiated Oxidation of Hydroxymethyl Hydroperoxide. *J. Phys. Chem. A* **2018**, *122* (30), 6292−6302.
(42) Zhou, S.; Joudan, S.; Forbes, M. W.; Zhou, Z.; Abbatt, J. P. D. Reaction of Condensed-Phase Criegee Intermediates with Carboxylic Acids and Perfluoroalkyl Carboxylic Acids. *Environ. Sci. Technol. Lett.* **2019**, *6*, 243−250.
(43) Qiu, J.; Ishizuka, S.; Tonokura, K.; Enami, S. Reactions of Criegee Intermediates with Benzoic Acid at the Gas/Liquid Interface. *J. Phys. Chem. A* **2018**, *122*, 6303−6310.
(44) Qiu, J.; Ishizuka, S.; Tonokura, K.; Colussi, A. J.; Enami, S. Reactivity of Monoterpene Criegee Intermediates at Gas−Liquid Interfaces. *J. Phys. Chem. A* **2018**, *122* (39), 7910−7917.
(45) Finlayson-Pitts, B. J.; Pitts, J. N. *Chemistry of the Upper and Lower Atmosphere*; Academic Press: San Diego, CA, 2000.
(46) Winterhalter, R.; Herrmann, F.; Kanawati, B.; Nguyen, T. L.; Peeters, J.; Vereecken, L.; Moortgat, G. K. The gas-phase ozonolysis of beta-caryophyllene ($C_{15}H_{24}$). Part I: an experimental study. *Phys. Chem. Chem. Phys.* **2009**, *11* (21), 4152−4172.
(47) Criegee, R. Mechanism of ozonolysis. *Angew. Chem., Int. Ed. Engl.* **1975**, *14*, 745−752.
(48) Witkowski, B.; Gierczak, T. Early stage composition of SOA produced by alpha-pinene/ozone reaction: alpha-Acyloxyhydroperoxy aldehydes and acidic dimers. *Atmos. Environ.* **2014**, *95*, 59−70.
(49) Neta, P.; Huie, R. E. Rate constants for reactions of nitrogen oxide (NO_3) radicals in aqueous solutions. *J. Phys. Chem.* **1986**, *90* (19), 4644−4648.
(50) Lakey, P. S.; Berkemeier, T.; Tong, H.; Arangio, A. M.; Lucas, K.; Pöschl, U.; Shiraiwa, M. Chemical exposure-response relationship between air pollutants and reactive oxygen species in the human respiratory tract. *Sci. Rep.* **2016**, *6*, 32916.
(51) Rissanen, M. P.; Kurtén, T.; Sipilä, M.; Thornton, J. A.; Kausiala, O.; Garmash, O.; Kjaergaard, H. G.; Petäjä, T.; Worsnop, D. R.; Ehn, M.; Kulmala, M. Effects of Chemical Complexity on the Autoxidation Mechanisms of Endocyclic Alkene Ozonolysis Products: From Methylcyclohexenes toward Understanding α-Pinene. *J. Phys. Chem. A* **2015**, *119* (19), 4633−4650.
(52) Anslyn, E. V.; Dougherty, D. *Modern Physical Organic Chemistry*; University Science Books: Sausolito, CA, 2005.
(53) Qiu, J.; Ishizuka, S.; Tonokura, K.; Sato, K.; Inomata, S.; Enami, S. Effects of pH on Interfacial Ozonolysis of α-Terpineol. *J. Phys. Chem. A* **2019**, *123*, 7148−7155.
(54) Zhou, X.; Lee, Y. N. Aqueous solubility and reaction kinetics of hydroxymethyl hydroperoxide. *J. Phys. Chem.* **1992**, *96* (1), 265−272.
(55) O'Brien, R. E.; Kroll, J. H. Photolytic Aging of Secondary Organic Aerosol: Evidence for a Substantial Photo-Recalcitrant Fraction. *J. Phys. Chem. Lett.* **2019**, *10*, 4003−4009.
(56) Enami, S.; Ishizuka, S.; Colussi, A. J. Chemical signatures of surface microheterogeneity on liquid mixtures. *J. Chem. Phys.* **2019**, *150* (2), 024702.
(57) Kononov, L. O. Chemical reactivity and solution structure: on the way to a paradigm shift? *RSC Adv.* **2015**, *5* (58), 46718−46734.
(58) Rak, D.; Sedlák, M. On the Mesoscale Solubility in Liquid Solutions and Mixtures. *J. Phys. Chem. B* **2019**, *123* (6), 1365−1374.
(59) Subramanian, D.; Boughter, C. T.; Klauda, J. B.; Hammouda, B.; Anisimov, M. A. Mesoscale inhomogeneities in aqueous solutions of small amphiphilic molecules. *Faraday Discuss.* **2014**, *167* (0), 217−238.
(60) Yinnon, C. A.; Yinnon, T. A. Domains in aqueous solutions: theory and experimental evidence. *Mod. Phys. Lett. B* **2009**, *23* (16), 1959−1973.
(61) Nagasaka, M.; Yuzawa, H.; Kosugi, N. Microheterogeneity in Aqueous Acetonitrile Solution Probed by Soft X-ray Absorption Spectroscopy. *J. Phys. Chem. B* **2020**, *124* (7), 1259−1265.
(62) Mukherjee, D.; Ortiz Rodriguez, L. I.; Hilaire, M. R.; Troxler, T.; Gai, F. 7-Cyanoindole fluorescence as a local hydration reporter: application to probe the microheterogeneity of nine water-organic binary mixtures. *Phys. Chem. Chem. Phys.* **2018**, *20* (4), 2527−2535.
(63) Krieger, U. K.; Marcolli, C.; Reid, J. P. Exploring the complexity of aerosol particle properties and processes using single particle techniques. *Chem. Soc. Rev.* **2012**, *41* (19), 6631−6662.
(64) Marsh, A.; Rovelli, G.; Song, Y.-C.; Pereira, K. L.; Willoughby, R. E.; Bzdek, B. R.; Hamilton, J.; Orr-Ewing, A.; Topping, D. O.; Reid, J. P. Accurate Representations of the Physicochemical Properties of

https://dx.doi.org/10.1021/acs.est.9b07497
Environ. Sci. Technol. 2020, 54, 3890−3899

Atmospheric Aerosols: When are Laboratory Measurements of Value? *Faraday Discuss.* **2017**, *200*, 639.
(65) Reid, J. P.; Dennis-Smither, B. J.; Kwamena, N.-O. A.; Miles, R. E.; Hanford, K. L.; Homer, C. J. The morphology of aerosol particles consisting of hydrophobic and hydrophilic phases: hydrocarbons, alcohols and fatty acids as the hydrophobic component. *Phys. Chem. Chem. Phys.* **2011**, *13* (34), 15559−15572.
(66) Fang, T.; Guo, H.; Zeng, L.; Verma, V.; Nenes, A.; Weber, R. J. Highly Acidic Ambient Particles, Soluble Metals, and Oxidative Potential: A Link between Sulfate and Aerosol Toxicity. *Environ. Sci. Technol.* **2017**, *51* (5), 2611−2620.
(67) Guo, H.; Sullivan, A. P.; Campuzano-Jost, P.; Schroder, J. C.; Lopez-Hilfiker, F. D.; Dibb, J. E.; Jimenez, J. L.; Thornton, J. A.; Brown, S. S.; Nenes, A.; et al. Fine particle pH and the partitioning of nitric acid during winter in the northeastern United States. *J. Geophys. Res. Atmos.* **2016**, *121* (17), 10355−10376.
(68) Bougiatioti, A.; Nikolaou, P.; Stavroulas, I.; Kouvarakis, G.; Weber, R.; Nenes, A.; Kanakidou, M.; Mihalopoulos, N. Particle water and pH in the eastern Mediterranean: source variability and implications for nutrient availability. *Atmos. Chem. Phys.* **2016**, *16* (7), 4579−4591.
(69) Witkowski, B.; Gierczak, T. Early stage composition of SOA produced by α-pinene/ozone reaction: α-Acyloxyhydroperoxy aldehydes and acidic dimers. *Atmos. Environ.* **2014**, *95*, 59−70.
(70) Shiraiwa, M.; Selzle, K.; Poschl, U. Hazardous components and health effects of atmospheric aerosol particles: reactive oxygen species, soot, polycyclic aromatic compounds and allergenic proteins. *Free Radical Res.* **2012**, *46* (8), 927−939.
(71) Shiraiwa, M.; Ueda, K.; Pozzer, A.; Lammel, G.; Kampf, C. J.; Fushimi, A.; Enami, S.; Arangio, A. M.; Fröhlich-Nowoisky, J.; Fujitani, Y.; et al. Aerosol health effects from molecular to global scales. *Environ. Sci. Technol.* **2017**, *51* (23), 13545−13567.
(72) Calvert, J. G.; Pitts, J. N. *Photochemistry*; Wiley: New York, 1966.

https://dx.doi.org/10.1021/acs.est.9b07497
Environ. Sci. Technol. 2020, 54, 3890−3899